THE JOURNAL OF PHYSICAL CHEMISTRY B

ARTICLE

pubs.acs.org/JPCB

Investigation on Metastable Solution of Cellulose Dissolved in NaOH/Urea Aqueous System at Low Temperature

Ang Lu,[†] Yating Liu,[†] Lina Zhang,[*,†] and Antje Potthast[‡]

[†]Department of Chemistry, Wuhan University, Wuhan 430072, P. R. China

[‡]Department of Chemistry, University of Natural Resources and Applied Life Sciences, Vienna, Austria

Supporting Information

ABSTRACT: Our previous work has demonstrated that the cellulose solution dissolved in 7 wt % NaOH/12 wt % urea aqueous system precooled to −12 °C was metastable. It is worth noting that light scattering investigation on the cellulose solution at metastable state is difficult. In the present paper, the solution properties and dynamic behaviors of cellulose dissolved in the NaOH/urea aqueous solution were investigated by means of dynamic light scattering (DLS), to confirm the influence factors of the DLS measurement. The DLS results revealed that, after the dispersion of cellulose in NaOH/urea at low temperature, the single cellulose inclusion complexes (ICs) coexisted with minor IC aggregates even in very dilute solution. With increasing cellulose concentration or system temperature or prolonging storage time, the IC aggregation increased, as a result of the occurrence of the imperfect urea shell and the reconstruction of the hydrogen bonds between cellulose chains. The cellulose solution was relatively stable at low concentration and low storage temperature and for short storage time. In this case, the single cellulose inclusion complexes were the predominant species, and coexisted with minor IC aggregates, which was better to be used to measure the cellulose solution with DLS.

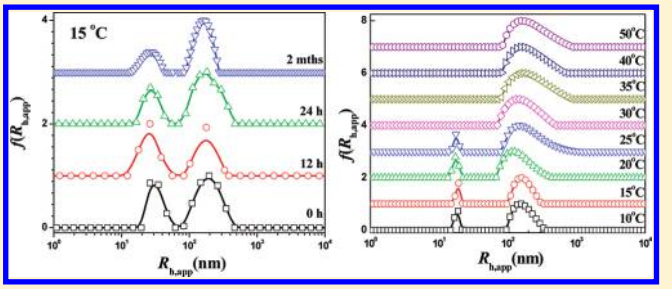

INTRODUCTION

In the 21st century, the wide utilization of renewable resources to produce environment-friendly materials has become a favorable international frontier which avoids using or producing any hazardous substances. However, as the most abundant natural resource, cellulose is difficult to dissolve in common solvent because of massive inter- and intramolecular hydrogen bonds.[1,2] Recently, new solvents of cellulose have been developed to dissolve cellulose under different conditions, such as *N*-methylmorpholine *N*-oxide (NMMO),[3] lithium chloride/*N*,*N*-dimethylacetamide (LiCl/DMAc),[4] and ionic liquids,[5] which dissolve cellulose at high temperature. In our laboratory, a new solvent system, including NaOH/urea, NaOH/thiourea, and LiOH/urea aqueous solutions has been developed to dissolve cellulose in 2 min at low temperature (−12 to −5 °C) rather than high temperature, in which an inclusion complex (IC) associated with water clusters, small solvent molecules, and cellulose macromolecules has been created to destroy the inter- and intramolecular hydrogen bonding of the native cellulose, leading to good dissolution.[6,7] Moreover, novel fibers have been spun from the cellulose dopes,[8] as well as a series of functional materials have been constructed from the cellulose solution dissolved at low temperature.[9−13] This solvent is an aqueous solution that is nonvolatile, nontoxic, and environmentally friendly, showing great potential in cellulose technology.[14] The rapid dissolution of cellulose at low temperature, which is quite attractive, arises as a result of the fast dynamic self-assembly process among small molecules in solution and the cellulose macromolecules.[6]

Dynamic self-assembly, as a metastable and random process,[15] is possible to control the dynamic self-assembly behavior by adjusting and controlling the external factors.[16] We have already demonstrated that a dynamic-assembly behavior of cellulose occurred in the dissolution process in NaOH/urea at low temperature;[6] it is hypothesized that the alternation of external factors can influence the cellulose dissolution condition. The investigation of the metastable behavior of the cellulose solution is very difficult. Therefore, it is necessary to study the influences of external factors on the cellulose solution, to supply useful information about the measurement, and to establish a fundamental basis for the further application of this novel cellulose technology. Therefore, dynamic light scattering (DLS) technique as a well-known tool for investigating the molecular self-assemble has been recruited in the present work. The intensity and polarization of light scattered from a polymer solution have been used to characterize the size, shape, and interaction of the particles in solution.[17,18] Furthermore, DLS is ideal to probe polymer behaviors in solution on nano scale.[19,20] DLS data can be obtained in situ,[21,22] and the molecular interpretation of data is straightforward.[23,24]

Received: July 13, 2011
Revised: September 12, 2011
Published: October 10, 2011

The aim of this work is to clarify dynamic behaviors and solution properties of cellulose in aqueous NaOH/urea system by static light scattering (SLS) and dynamic light scattering as well as by transmission electron microscopy (TEM) induced by the external factors. The influences of concentration, system temperature, and storage time on the stability of the cellulose solution and IC structure were studied and discussed. We hope to provide useful information on the determination of the solution properties for cellulose dissolved in NaOH/urea at low temperature.

EXPERIMENTAL SECTION

Materials. Cellulose (cotton linter pulps) with a α-cellulose content of more than 95% was supplied by Hubei Chemical Fiber Co. Ltd. (Xiangfan, China). Its weight-average molecular weight (M_w) was determined in 4.6 wt % LiOH/15.0 wt % urea aqueous solution with laser light scattering to be 11.0×10^4 g/mol.[25] The cellulose sample was vacuum-dried at 55 °C for 24 h to remove any moisture before use. Commercially available sodium hydroxide (NaOH) and urea were of analytical grade (Shanghai Chemical Reagent Co., China), and were used without further purification.

Preparation of Cellulose Solution. A mixture of aqueous solution as solvent for cellulose was prepared by directly mixing NaOH, urea and distilled water with NaOH:urea:H_2O of 7:12:81 by weight. The solvent was stored at about 0 °C before use. To obtain a dilute solution, desired amount cellulose was dispersed in the solvent. The resultant solution was precooled in a refrigerator to −12 °C, and then stirred in a 15 °C water bath for 5 min. The cellulose solution was filtered through a 0.45 μm Millipore filter to purify. The cellulose solution was used immediately for tests without delay (hereafter referred to as *fresh* solution in this study) in order to exclude the effect of storage time. To correct the cellulose concentration, a stoichiometric amount of 1 M HCl was used to neutralize the NaOH component and to precipitate the cellulose. The exact concentration of the cellulose in NaOH/urea aqueous solution was determined from the weight of the precipitated cellulose.

Characterization. Static and dynamic light scatterings (SLS and DLS) were used to characterize the molecular weight and chain conformation of cellulose in the dilute solution (NaOH/urea aqueous system). A modified commercial light scattering spectrometer (ALV/SP-125, ALV, Germany) equipped with an ALV-5000/E multi-τ digital time correlator and a He−Ne laser (at λ = 632.8 nm) was used at scattering angle θ of 30°. All of the cellulose solutions were prepared and made optically clean by filtration through 0.45 μm Millipore filters. A Zimm plot was used to calculate the weight-average molecular weight (M_w) and the radius of gyration ($\langle R_g^2\rangle^{1/2}$). The CONTIN program[26] was used for the analysis of dynamic light-scattering data. The hydrodynamic radius (R_h) was calculated by using the Stokes−Einstein relation as

$$R_h = k_B T/6\pi\eta_0 D \quad (1)$$

where k_B is the Boltzmann constant, T the temperature in units of K, η_0 the solvent viscosity, and D the translational diffusion coefficient. The light scattering experiments were repeated several times, and the results were reproducible. Intrinsic viscosity of the cellulose solution was measured with an Ubbelohde viscometer, and the viscosity of cellulose solution was measured with an ARES-RFS III rheometer (TA Instruments, USA) by a model fitting. Furthermore, the results showed that the viscosity change in temperature range from 5 to 50 °C was negligible for both the solvent and the dilute cellulose solution.

Static light scattering measurements was also operated. In static LS, the excess scattered intensity $I(q)$ with respect to the solvent was measured, and the magnitude of the scattering wave vector q is given by

$$q = |\vec{q}| = 4\pi n_0 \sin(\theta/2)/\lambda_0 \quad (2)$$

where n is the refractive index of the solvent, λ_0 is the wavelength of light in the vacuum, and θ is the scattering angle. In our experiments, θ was varied between 30 and 150°, which corresponded to q in the range from 6.8×10^{-3} to 2.6×10^{-2} nm^{-1}. The refractive index increment (dn/dc) was determined by a novel and precise differential refractometer combined with the results by fluorescence labeling with gel permeation chromatography obtained in University of Natural Resources and Applied Life Sciences, Vienna, Austria:[27,28] UV spectra were obtained on a Hitachi U-3010 photometer in quartz cuvettes (d = 1 cm) at 20 °C and fluorescence spectra on a Hitachi F-4500 device under otherwise identical conditions. GPC and high-performance liquid chromatography (HPLC) measurements used the following components: online degasser, Dionex DG-2410 and Gynkotek DG-1310; pumps, Dionex P580 (HPLC), Kontron 420 (GPC); pulse damper; autosampler, HP series 1100; column oven, Gynkotek STH 585; fluorescence detector, TSP FL2000; multiple-angle laser light scattering (MALLS) detector, Wyatt Dawn DSP with argon ion laser (λ_0 = 488 nm), refractive index (RI) detector, Shodex RI-71; and UV detector, Dionex UVD 340. Data evaluation was performed with standard Chromeleon and Astra software. We have finally confirmed the closest dn/dc of cellulose in NaOH/urea aqueous soluion to be 0.170, according to the dates of our own and from Vienna (see Supporting Information).

Corrections to the absolute time-averaged scattering intensities $R_{vv}(q)$ (excess Rayleigh ratio) were made using a toluene sample reference, for which the excess Rayleigh ratio is given as follows:

$$R_{vv}(q) = \{[\langle I_{solusion}(q)\rangle - \langle I_{solvent}(q)\rangle] / \langle I_{ref}(q)\rangle\} R_{ref} (n_{solvent}/n_{ref})^2 \quad (3)$$

where $R_{vv}(q)$ of a dilute polymer solution at concentration c (g/mL) is related to the weight-average molecular weight (M_w). From static light scattering data, the M_w, the second virial coefficient A_2 and the z-average radius of gyration $\langle R_g^2\rangle^{1/2}$ (or written as $\langle R_g\rangle$) can be obtained by[29]

$$Kc/R_{vv}(q) = (1 + \langle R_g^2\rangle q^2/3)/M_w + 2A_2 c \quad (4)$$

where $K = 4\pi^2 n^2 (dn/dc)^2/(N_A \lambda_0^4)$, with N_A, n, and λ_0 being Avogadro's constant, the solvent refractive index, and the wavelength of light in vacuum, respectively. $q = (4\pi n/\lambda_0)\sin(\theta/2)$, θ being the scattering angel. It is noted that a combination of static and dynamic LLS results is able to provide information on the aggregation number, and the weight fraction of the aggregates in the solution.[30,31] The following is the outline of its basic principle. On the basis of eq 4, at $t \to 0$, $q \to 0$, and a finite c, we have

$$|g^{(1)}(0,q)| = \int_0^\infty G(\Gamma)\, d\Gamma \propto \langle I\rangle \propto R_{vv}(q \to 0) \propto M^*_w c \quad (5)$$

where M^*_w [$=M_w(1 - 2A_2M_wc)$] is an apparent weight-average molecular mass at a finite c.[32,33] Equation 5 shows that the peak area in $G(\Gamma)$ is proportional to the excess scattered intensity.

Transmission electron microscopy (TEM) observation of the molecular morphology of cellulose in aqueous NaOH/urea solution was carried out on a JEM-2010 (HT) transmission electron microscope (JEOL TEM, Japan). A thin layer of the dilute cellulose solution was suspended on a holey carbon film, which was supported on a copper grid. The specimen was dried in air at ambient temperature and pressure for 20 min and was then imaged at an accelerating voltage of 200 kV. Relative viscosities (η_r) of the cellulose in NaOH/urea aqueous solution were measured at 25 ± 0.1 °C using an Ubbelohde capillary viscometer. The kinetic energy correction was always negligible.

RESULTS AND DISCUSSION

Stability of Cellulose Inclusion Complexes in NaOH/Urea System. In previous work, the results from ^{13}C NMR, ^{15}N NMR, ^{1}H NMR, FT-IR, TEM, small-angle neutron scattering, and wide-angle X-ray diffraction have confirmed that NaOH "hydrates" can be more easily attracted to cellulose chains through the formation of new hydrogen-bonded networks in the cellulose−NaOH/urea system at low temperatures.[6] Moreover, the urea hydrates can be self-assembled on the surface of the NaOH hydrogen-bonded cellulose to form an inclusion complex (IC), leading to the dissolution of cellulose. In the dilute solution, IC existed as wormlike conformation, supported by dynamic and static light scattering, as well as TEM.[6] Thus, IC associated with small solvent molecules, cellulose chains, and water clusters has been created in cellulose/NaOH/urea system at low temperature to destroy the inter- and intramolecular hydrogen bonding of native cellulose, leading to good dissolution. The urea mainly contributed as the IC shell to prevent the self-association of cellulose in the solution. However, the individual cellulose ICs could link with each other, forming IC aggregates, as a result of the occurrence of imperfect shell of the IC.[6] These results indicated that the IC structure was unstable, namely, it would be influenced by external factors.

Prior to investigating the dynamic structure of the cellulose in NaOH/urea, we tested the cellulose solution stability on the whole by viscosity. Figure 1 shows the relative viscosity (η_r) of cellulose solution as a function of both time and temperature. The cellulose solution at low temperature exhibited higher η_r than at high temperature during the tested time range. The results indicated the cellulose solution in the NaOH/urea system was more stable at relatively low temperature and displayed a more extended chain conformation than at higher temperature, and was also significantly more stable than that of cuprammonium.[34] A loss in the η_r was observed for the tested temperatures, and the loss was smaller at lower temperature than at the higher one. The loss in η_r can be assigned to a reassociation of the cellulose chains, and the results suggested that this cellulose chain reassociation was much easier induced at higher temperature. In this case, *fresh* solution was applied for the dynamic light scattering measurement in order to exclude the negligible time influences for precision, except the storage time influence measurements.

Effects of Scattering Angle. The hydrodynamic radius of wormlike chains would depend on the scattering angle.[35] Figure 2 shows the angle dependence of autocorrelation function and particle size distribution of 0.110 g/L cellulose in NaOH/urea at

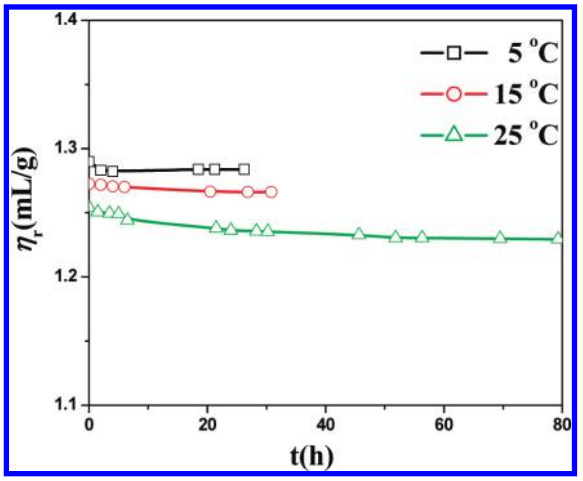

Figure 1. Relative viscosity vs time of the cellulose in NaOH/urea aqueous solution at different temperatures.

15 °C. The intercept at $t = 0$ of $g^2(q)$ is smaller than unity, indicating a significant heterodyne scattering. The corresponding hydrodynamic radius distributions were calculated from the CONTIN analysis. The autocorrelation function shifted with q, and the $g^2(t)$ at different angles nearly overlapped each other when plotted as a function of k^2t, where $k = (4\pi n/\lambda)\sin(q/2)$ was the scattering wave vector (not shown), indicating a slight rotational diffusional behavior of cellulose in NaOH/urea system. This could be explained by the formation and destruction of ICs, namely, the ICs were in metastable state. Thus, the contribution of the rotational diffusion to the autocorrelation functions weakened significantly. In Figure 2, the peak at about 30 nm can be assigned to single cellulose inclusion complex, which was associated with cellulose and NaOH, urea and water through hydrogen-bonded networks at low temperature, and the larger dimension peak was assigned to IC aggregates. In the angle range from 30 to 90°, single IC coexisted with IC aggregates. The peak position of both components did not move much while the tested angles varied from 30 to 90°. However, the two well-separated peaks connected with each other at relatively high tested angles. There was a tiny shift to a smaller diameter with an increasing scattering angle, indicating that aggregates have a size distribution.[36] The system was at metastable state, and the formation and destruction of ICs led to the weakness of the rotation diffusion contribution to the autocorrelation function. Therefore, the DLS data at 30° were used here.

Effects of Cellulose Concentration. Figure 3 shows the concentration dependence of particle size distribution of cellulose in NaOH/urea at 15 °C, where the corresponding hydrodynamic radius distribution was calculated from the CONTIN analysis. Even in the very dilute concentration (0.153 g/L), the cellulose solution exhibited two peaks corresponding to single ICs and IC aggregates, respectively. An imperfect shell consisting of NaOH hydrate and urea hydrate appeared in the IC structure, leading to aggregation as a result of the aggregation trend of exposed hydroxyls of cellulose. The area (A) under each peak reflects directly the scattering intensity from DLS, which is related with molecular mass (M) and weight fraction (w) of macromolecules. The w value of each component including single chain and aggregates can be estimated by

$$A_1:A_2 = w_1M_1:w_2M_2 \quad (6)$$

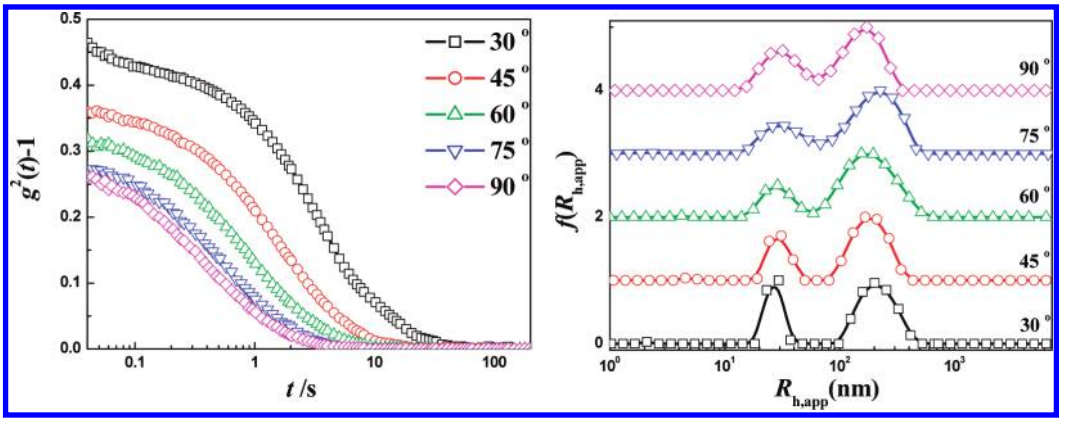

Figure 2. Angle dependence of autocorrelation function and of particle size distribution of 0.110 g/L cellulose in NaOH/urea at 15 °C, where the corresponding hydrodynamic radius distributions were calculated from the CONTIN analysis.

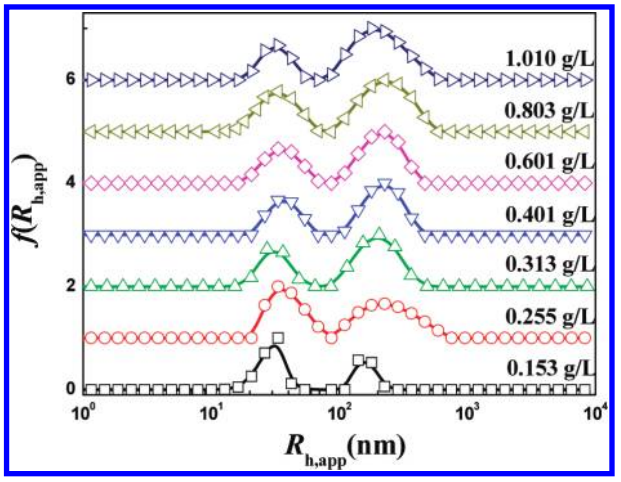

Figure 3. Concentration dependence of particle size distribution of cellulose in NaOH/urea at 15 °C, where the corresponding hydrodynamic radius distributions were calculated from the CONTIN analysis.

where subscripts 1 and 2 represent two kinds of the components and $w_1 + w_2 = 1$. Usually, M was in direct proportion to R_h. Analysis of Figure 3 and eq 6 suggested that the aggregate should be much less than single IC in the dilute cellulose solution at 15 °C. The predominant species in the cellulose dilute solution at the testing temperature was single IC, which coexisted with the IC aggregates here. However, when the concentration increased to 0.313 g/L, the IC aggregates obtained a larger proportion than the single ICs. It can be explained that the amount of cellulose chains in the solution increased, and cellulose chains obtained much more probability to contact with each other, leading to aggregations. Furthermore, compared with the 0.153 g/L cellulose solution, the IC aggregates peaks at higher concentrations exhibited much broader distribution. It was noted that the two peaks of the 0.153 g/L cellulose solution can be well divided; however, the two peaks gradually connected with each other as the concentration further increased, indicating an existence of a medium dimension between single ICs and IC aggregations. There was equilibrium of IC association to aggregates and IC aggregation disassociating to single ICs in the cellulose solution. In very dilute solutions, the ICs or IC aggregations were separated from each other and there were no interactions between them. As concentration increased, they could contact with each other much easier, and that led to much more interactions. As a result, the equilibrium of IC association and IC aggregation disassociation had been partly destroyed, and the medium dimension distribution appeared and was tested by DLS.

Figure 4 shows the concentration dependence of particle size distribution of cellulose in NaOH/urea at 10 and 25 °C, where the corresponding hydrodynamic radius distributions were calculated from the CONTIN analysis. The cellulose solution at 10 and 25 °C basically exhibited a similar rule with the solution at 15 °C. It was noted that the proportion of the two peaks varied with temperatures: at high temperature, the proportion of IC aggregates was much larger than at relatively low temperature. The cellulose IC structure was most stable at relatively low temperature, whereas at higher temperatures the IC structure would be destroyed as a result of the imperfect shell, then exposed hydroxyls on the cellulose chains dominated the self-association trend, leading to the further association of partly destroyed ICs.[6] That is, the cellulose solution at 25 °C had larger proportion of aggregations than at 10 and 20 °C, indicating more single ICs transferred into aggregations. Therefore, the cellulose dilute solution was more stable at 15 °C than at 25 °C.

Effects of Storage Time. Figure 5 shows the time dependence of particle size distribution of cellulose in NaOH/urea with a 0.470 g/L concentration at 15 and 25 °C, where the corresponding hydrodynamic radius distributions were calculated from the CONTIN analysis. At 15 °C, there was no shift of the main peaks, and after storage for a long time, the cellulose solution still consisted of single ICs and IC aggregates, further indicating that the cellulose solution was relatively stable at this temperature. However, with the storage process, the proportion of IC aggregates increased, indicating the single ICs gradually associated into aggregates, as a result of the occurrence of the imperfect shell of the ICs with an increase of the storage time, because of the external factors caused by self-association trend of cellulose. The solution stored at 25 °C showed a similar property: after storing for 24 h, the proportion of IC aggregates increased a lot, indicating the association of single ICs. Moreover, the alteration in 24 h of cellulose solution at 25 °C was far greater than that at 15 °C, indicating high temperature could accelerate the association of single ICs into IC aggregates, which was in accordance with Figure 1.

In order to provide straightforward evidence for the aggregation change of the ICs in NaOH/urea system with concentration

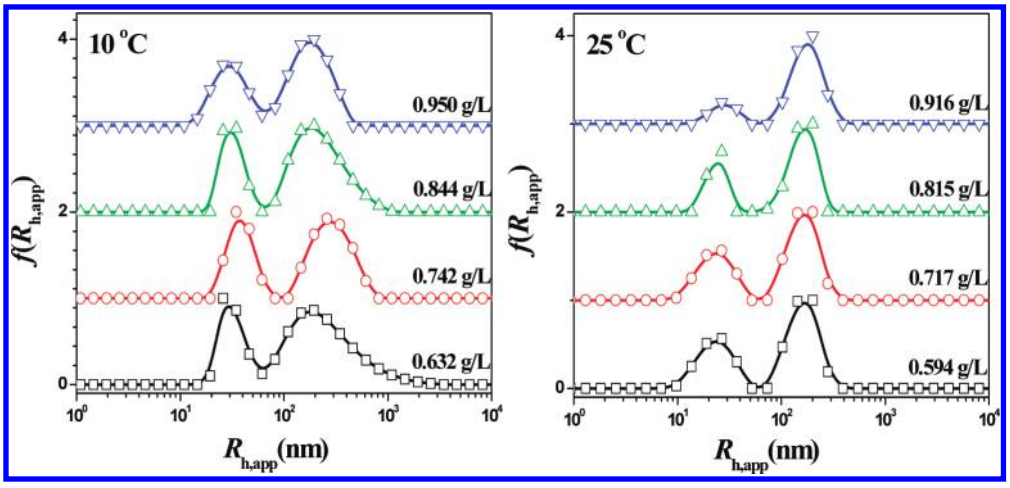

Figure 4. Concentration dependence of particle size distribution of cellulose in NaOH/urea at 10 and 25 °C, where the corresponding hydrodynamic radius distributions were calculated from the CONTIN analysis.

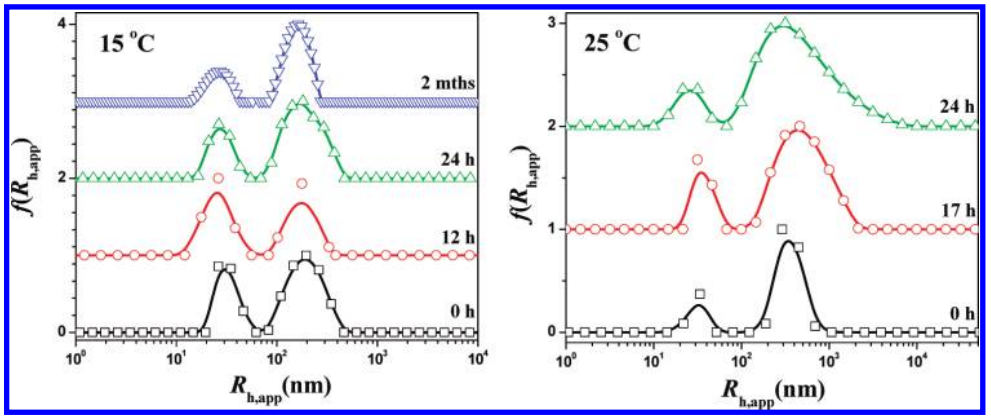

Figure 5. Time dependence of particle size distribution of cellulose in NaOH/urea with a 0.470 g/L concentration at 15 and 25 °C, where the corresponding hydrodynamic radius distributions were calculated from the CONTIN analysis.

and storage time, TEM was applied to observe the morphology of ICs. TEM images of the cellulose dilute solutions with different concentration and storage time are shown in Figure 6. The ICs composed of cellulose, NaOH, urea, and water clusters displayed a wormlike shape, which presented a kebab shape rather than a homogeneous surface because the electron beam struck the nonmetal sample, resulting in the partial melting of urea on the surface of ICs. The urea mainly contributed as the IC shell to prevent the self-association of cellulose in the solution. Interestingly, with increasing concentration of the cellulose solution in the NaOH/urea system, the individual cellulose ICs could link with each other, forming IC aggregates or thin film as shown in Figure 6d.

Figure 7 shows the Zimm plot of fresh cellulose solution and cellulose solution stored for 24 h at 15 and 25 °C, and the relative M_w, R_g, and A_2 are summarized in Table 1. Compared with 15 °C, the Zimm plot at 25 °C exhibited a deformation at small angles, indicating an existence of intensive large aggregates. However, the Zimm plot at 10 °C exhibited an ordinary polymer solution properties. From Table 1, the M_w of fresh cellulose solution at 15 °C was higher than 11.0×10^4 g/mol, indicating the predominant species in the cellulose dilute solution was a single IC, which coexisted with the IC aggregates. After 24 h storage, the R_g and M_w both increased, indicating an increase of the IC aggregates proportion. A similar rule can be found for the cellulose solution at 25 °C, and after 24 h storage, the amplifications of M_w and R_g were much larger than that at 15 °C, in which the high temperature induced the intensively aggregation of single ICs. Moreover, the M_w and R_g of fresh cellulose solution at 25 °C were larger than that at 15 °C, further demonstrating the conclusion that single ICs more easily associated with each other to form aggregates at higher temperature.

Effects of Temperature. Figure 8 shows the temperature dependence of particle size distribution of cellulose in NaOH/urea with $c = 0.301$ g/L, where the corresponding hydrodynamic radius distributions were calculated from the CONTIN analysis. The cellulose solution exhibited two peaks in the low-temperature range from 10 to 25 °C, corresponding to single ICs and IC aggregates, respectively. Moreover, as the temperature increased from 10 to 25 °C, the single ICs proportion gradually decreased while the proportion of the IC aggregates increased a lot, and the distribution of IC aggregates also enlarged. This indicated that single ICs associated to form larger aggregates as temperature increased. When the temperature reached 30 °C, there was only one peak in the cellulose solution assigned to IC aggregates, indicating the single ICs were totally transferred into aggregates.

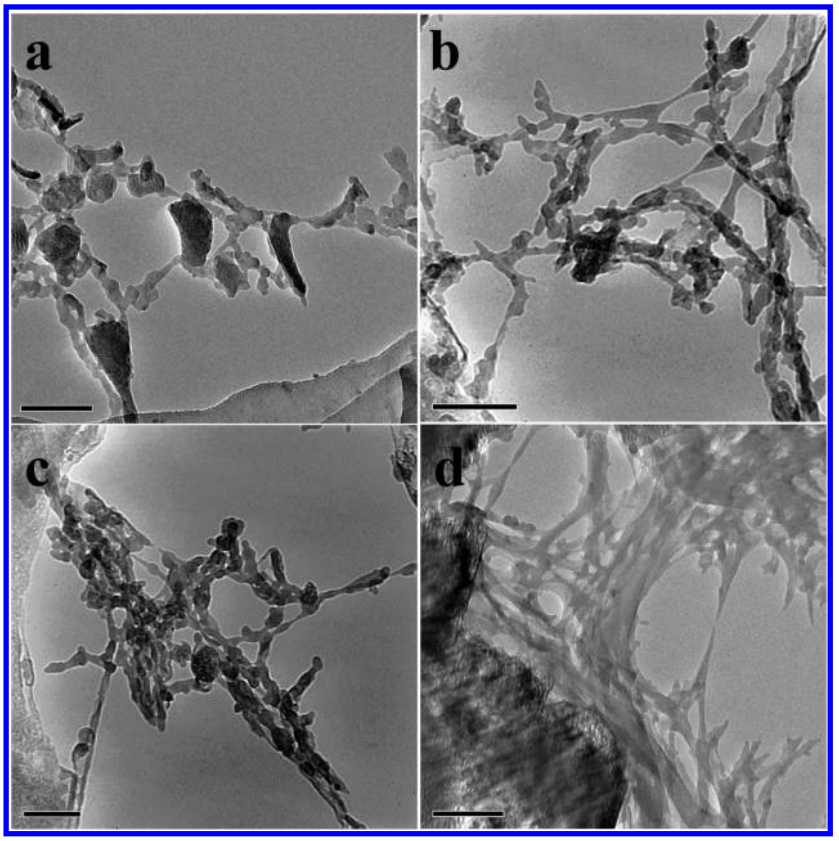

Figure 6. TEM images of the cellulose dilute solutions with increase of concentration from (a) to (d). The scale bar is 100 nm.

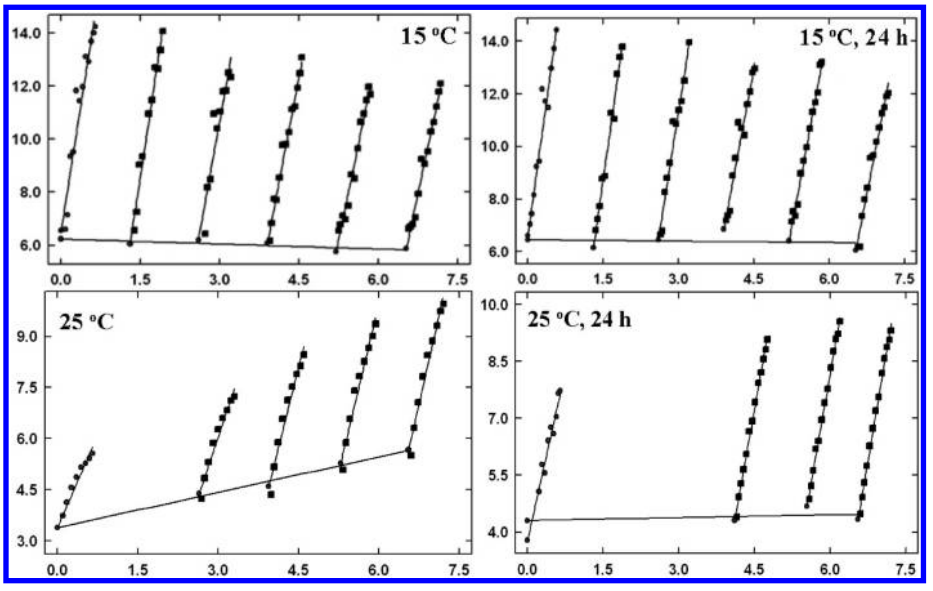

Figure 7. Zimm plots of cellulose in NaOH/urea aqueous solution at different temperatures.

With further increase in the temperature, the distribution of aggregate peak further enlarged, indicating the formation of much larger dimension clusters. At high temperatures, the IC structure would be entirely destroyed, and the exposed hydroxyls of the cellulose chains would interact with each other through hydrogen bonding into larger clusters, whose dimension could be 1000 nm according to Figure 8. And these clusters would not form ICs again even if we decreased the temperature to 10 °C.

In view of the above results, the cellulose IC structures were not stable and the cellulose solution would be perturbed by external factors. Even at very low concentrations, the cellulose in NaOH/urea system exhibited two peaks corresponding to single ICs and IC aggregates. As a result of the imperfect shell of ICs,

Table 1. Static Light Scattering Results of Cellulose in NaOH/Urea Aqueous Solution

T	M_w ($\times 10^4$ g·mol^{-1})	R_g (nm)	A_2 (cm^{-3}·mol·g^{-2})
15 °C	13.87	68.76	1.648×10^{-7}
15 °C, 24 h	15.96	71.25	-3.847×10^{-7}
25 °C	33.12	71.64	2.592×10^{-6}
25 °C, 24 h	45.14	144.5	2.629×10^{-6}

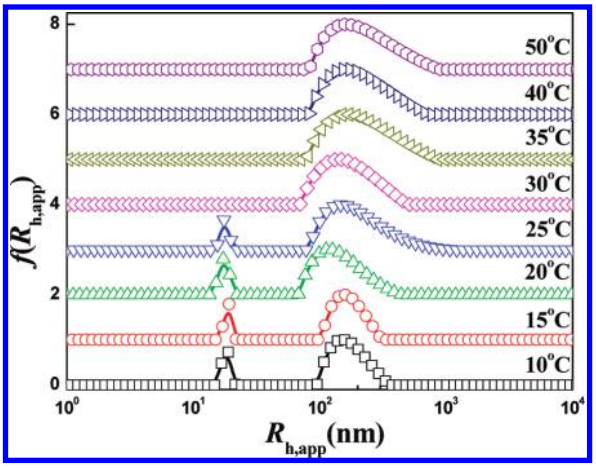

Figure 8. Temperature dependence of particle size distribution of cellulose in NaOH/urea with c = 0.301 g/L, where the corresponding hydrodynamic radius distributions were calculated from the CONTIN analysis.

the single ICs would associate with each other to form aggregates. Similar results had also been reported for some other cellulose solvents systems.[37−40] There was equilibrium between ICs associating with aggregates and IC aggregation disassociating to single ICs in the cellulose solution. With increasing cellulose concentrations, the amount of cellulose chains increased and the rate of ICs contacted with each other also rose, leading to aggregations of ICs in the cellulose solution. That was the reason for IC aggregates proportion increasing with concentration, and in this concentration increasing process, the IC structures were relatively stable; i.e., the aggregation of ICs was caused by the increasing contact rate between the ICs. However, temperature had different effects on the cellulose solution from concentration. As shown in Figure 8, the curve varied a lot with temperature increasing from 10 to 50 °C, and finally the single ICs peak vanished. In the heating process, the imperfect shell of IC structure was gradually destroyed as IC was most stable at low temperature. After that, the exposed hydroxyls of the cellulose associated with each other via hydrogen bonding and formed large dimension clusters, which was demonstrated by the long tail of the 50 °C curve in Figure 8. The storage time had a similar effect with the temperature, as shown in Figure 5. For the storage at 15 °C, the curve did not vary much after 24 h, and after 2 months, there was an obvious transform from single ICs to IC aggregates, indicating the IC structure (shell of the IC) was destroyed in the period. However, the storage at 25 °C showed much differences, and the curve varied a lot after only 24 h, indicating the temperature had a much strong promotion effect on the destruction of the IC structure. From the above, the cellulose solution would be perturbed by external factors, such as polymer concentration, system temperature, and storage time. Increase of concentration, temperature, and time would lead to the single ICs associating into IC aggregates; however, the reasons were not the same: increasing concentration increased the contact rate between the ICs, and higher temperature or longer time both would destroy the IC structure.

However, the IC structure associated with cellulose, NaOH, urea, and water clusters has been not clarified well, and we will study the crystal structure of cellobiose and cellulose oligomers in NaOH/urea to investigate the IC structures. We hope to supply useful information on this amazing technique.

CONCLUSIONS

Formation of cellulose inclusion complexes (ICs) surrounded by urea shell in aqueous NaOH/urea at low concentration through a dynamic self-assembly process led to a good dissolution. The cellulose solution was metastable in the solvent. The external factors, such as storage time, cellulose concentration, and system temperature changes could destroy the IC structure, leading to the cellulose IC aggregates. With an increase of cellulose concentration, temperature, or storage time, the proportion of IC aggregates enlarged as a result of imperfect shell of IC structure, indicating single ICs were transferred into aggregates with increase of the polymer concentration, system temperature, and storage time. Therefore, measurements and investigation on properties of the cellulose dilute solution with light scattering should be performed under considerate conditions to avoid the aggregation phenomenon. The cellulose solution was relatively stable at low concentration, low storage temperature, and short storage time. In this case, the single cellulose inclusion complexes were the predominant species and coexisted with minor IC aggregates.

ASSOCIATED CONTENT

Supporting Information. The confirmation of dn/dc of cellulose in NaOH/urea system is demonstrated in figures. This material is available free of charge via the Internet at http://pubs.acs.org.

AUTHOR INFORMATION

Corresponding Author

*E-mail: lnzhang@public.wh.hb.cn. Tel.: +86-27-87219274. Fax: +86-27-68754067.

ACKNOWLEDGMENT

This work was supported by National Basic Research Program of China (973 Program, 2010CB732203) and the National Natural Science Foundation of China (20474048 and 20874079).

REFERENCES

(1) Klemm, D.; Heublein, B.; Fink, H.-P.; Bohn, A. *Angew. Chem., Int. Ed.* **2005**, *44*, 3358–3393.

(2) Yan, L.; Chen, J.; Bangal, P. R. *Macromol. Biosci.* **2007**, *7*, 1139–1148.

(3) Maia, E.; Perez, S. *Nouv. J. Chim.* **1983**, *7*, 89.

(4) Dawsey, T. R.; McCormick, C. L. *J. Macromol. Sci. Rev. Macromol. Chem. Phys.* **1990**, *C30*, 405–431.

(5) Swatloski, R. P.; Spear, S. K.; Holbrey, J. D.; Rogers, R. D. *J. Am. Chem. Soc.* **2002**, *124*, 4974–4975.

(6) Cai, J.; Zhang, L.; Liu, S.; Liu, Y.; Xu, X.; Chen, X.; Chu, B.; Guo, X.; Xu, J.; Cheng, H.; Han, C. C.; Kuga, S. *Macromolecules* **2008**, *41*, 9345–9351.
(7) Cai, J.; Zhang, L. *Biomacromolecules* **2006**, *7*, 183–189.
(8) Cai, J.; Zhang, L.; Zhou, J.; Qi, H.; Chen, H.; Kondo, T.; Chen, X.; Chu, B. *Adv. Mater.* **2007**, *19*, 821–825.
(9) Luo, X.; Zhang, L. *Biomacromolecules* **2010**, *11*, 2896–2903.
(10) Chang, C.; Peng, J.; Zhang, L.; Pang, D. *J. Mater. Chem.* **2009**, *19*, 7771–7776.
(11) Liu, S.; Zhang, L.; Zhou, J.; Xiang, J.; Sun, J.; Guan, J. *Chem. Mater.* **2008**, *20*, 3623–3628.
(12) Luo, X.; Liu, S.; Zhou, J.; Zhang, L. *J. Mater. Chem.* **2009**, *19*, 3538–3545.
(13) Qi, H.; Cai, J.; Zhang, L.; Kuga, S. *Biomacromolecules* **2009**, *10*, 1597–1602.
(14) http://cell.sites.acs.org/
(15) Whitesides, G. M.; Grzybowski, B. A. *Science* **2002**, *295*, 2418–2421.
(16) Fialkowski, M.; Bishop, K. J. M.; Klajn, R. *J. Phys. Chem. B* **2006**, *110*, 2482–2496.
(17) Zulfiqar, S.; Ishaq, M.; Ahmad, Z. *Polym. Adv. Technol.* **2008**, *19*, 1250–1255.
(18) Zhang, G. *Macromolecules* **2004**, *37*, 6553–6557.
(19) Siu, M.; Zhang, G.; Wu, C. *Macromolecules* **2002**, *35*, 2723–2727.
(20) Zhao, J.; Zhang, G.; Pispas, S. *J. Phys. Chem. B* **2009**, *113*, 10600–10606.
(21) Zhang, G.; Wu, C. *J. Am. Chem. Soc.* **2001**, *123*, 1376–1380.
(22) Buhler, E.; Rinaudo, M. *Macromolecules* **2000**, *33*, 2098–2106.
(23) Kanzaki, N.; Taro, Q.; Uyeda, P.; Onuma, K. *J. Phys. Chem. B* **2006**, *110*, 2881–2887.
(24) Lin, W.; Zhou, Y. S.; Wu, C. *Macromolecules* **2002**, *35*, 7407–7413.
(25) Cai, J.; Liu, Y.; Zhang, L. *J. Polym. Sci. Part B* **2006**, *44*, 3093–3101.
(26) Chu, B. *Laser Light Scattering*, 2nd ed.; Academic Press: New York, 1991.
(27) Röhrling, J.; Potthast, A.; Rosenau, T.; Lange, T.; Ebner, G.; Sixta, H.; Kosma, P. *Biomacromolecules* **2002**, *3*, 959–968.
(28) Bohrn, R.; Potthast, A.; Schiehser, S.; Rosenau, T.; Sixta, H.; Kosma, P. *Biomacromolecules* **2006**, *7*, 1743–1750.
(29) Zimm, B. H. *J. Chem. Phys.* **1948**, *16*, 1099–1116.
(30) Wu, C.; Mohammad, S.; Woo, K. F. *Macromolecules* **1995**, *28*, 4914–4919.
(31) Kirill, N. B.; Iwao, T.; William, J. M.; Frank, E. K. *Macromolecules* **1993**, *26*, 1972–1974.
(32) Yamakawa, H. *Modern Theory of Polymer Solutions*; Harper & Row: New York, 1971.
(33) Sato, T.; Jinbo, Y.; Teramoto, A. *Polym. J.* **1995**, *27*, 384–387.
(34) Zhou, J.; Zhang, L. *Polym. J.* **2000**, *32*, 866–870.
(35) Lin, M.; Lindsay, H.; Weitz, D.; Klein, R.; Ball, R.; Meakin, P. *J. Phys.: Condens. Matter* **1990**, *2*, 3093–3113.
(36) Chakraborty, S.; Sahoo, B.; Teraoka, I.; Gross, R. A. *Carbohydr. Polym.* **2005**, *60*, 475–481.
(37) Schulz, L.; Seger, B.; Buchard, W. *Macromol. Chem. Phys.* **2000**, *201*, 2008–2022.
(38) Morgenstern, B.; Röder, T. *Papier* **1998**, *52*, 713–717.
(39) Fischer, K. *Papier* **1994**, *48*, 769–774.
(40) Chen, X.; Burger, C.; Wan, F.; Zhang, J.; Rong, L.; Hsiao, B. S.; Chu, B.; Cai, J.; Zhang, L. *Biomacromolecules* **2007**, *8*, 1918–1926.